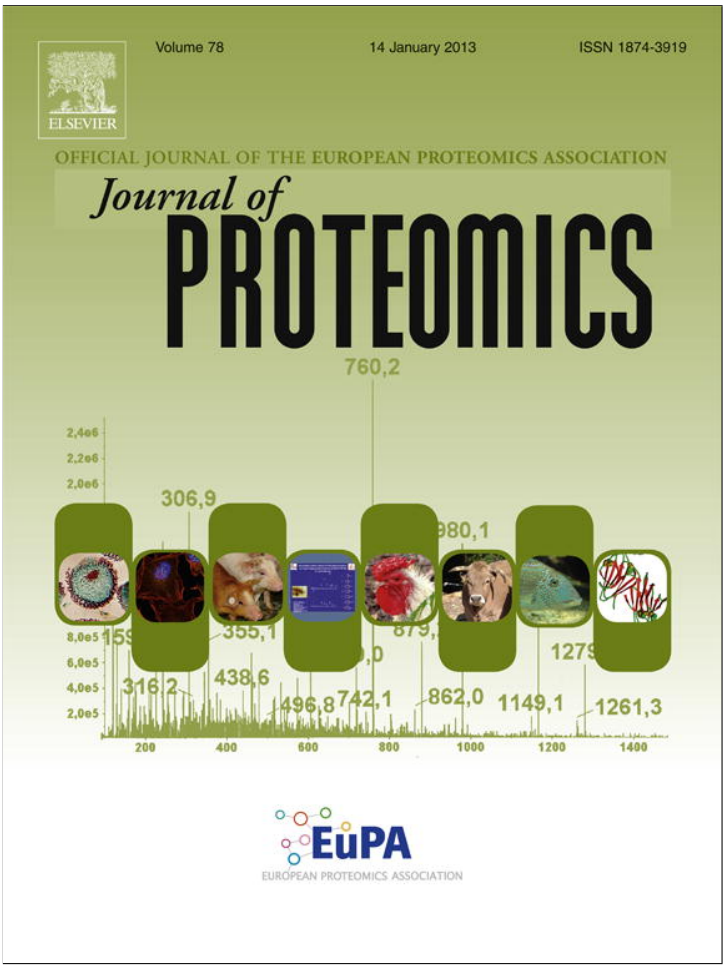

JOURNAL OF PROTEOMICS 78 (2013) 461–476

Available online at www.sciencedirect.com

SciVerse ScienceDirect

www.elsevier.com/locate/jprot

Proteomic changes in *Actinidia chinensis* shoot during systemic infection with a pandemic *Pseudomonas syringae* pv. *actinidiae* strain

Milena Petriccione[a], *Ilaria Di Cecco*[a], *Simona Arena*[b], *Andrea Scaloni*[b,*], *Marco Scortichini*[a,c,**]

[a]*Research Unit for Fruit Trees, Agricultural Research Council (CRA), 81100 Caserta, Italy*
[b]*Proteomics and Mass Spectrometry Laboratory, ISPAAM, National Research Council, 80147 Naples, Italy*
[c]*Research Centre for Fruit Crops, Agricultural Research Council (CRA), 00134 Rome, Italy*

ARTICLE INFO

Article history:
Received 19 July 2012
Accepted 14 October 2012
Available online 23 October 2012

Keywords:
Proteomics
Kiwifruit
Pseudomonas syringae
Plant–microbe interaction
Biotic stress

ABSTRACT

A pandemic, very aggressive population of *Pseudomonas syringae* pv. *actinidiae* is currently causing severe economic losses to kiwifruit crops worldwide. Upon leaf attack, this Gram-negative bacterium systemically reaches the plant shoot in a week period. In this study, combined 2-DE and nanoLC-ESI-LIT-MS/MS procedures were used to describe major proteomic changes in *Actinidia chinensis* shoot following bacterial inoculation in host leaf. A total of 117 differentially represented protein spots were identified in infected and control shoots. Protein species associated with plant defence, including type-members of the plant basal defence, pathogenesis, oxidative stress and heat shock, or with transport and signalling events, were the most represented category of induced components. Proteins involved in carbohydrate metabolism and photosynthesis were also augmented upon infection. In parallel, a bacterial outer membrane polypeptide component was identified in shoot tissues, whose homologues were already linked to bacterial virulence in other eukaryotes. Semiquantitative RT-PCR analysis confirmed expression data for all selected plant gene products. All these data suggest a general reprogramming of shoot metabolism following pathogen systemic infection, highlighting organ-specific differences within the context of a general similarity with respect to other pathosystems. In addition to present preliminary information on the molecular mechanisms regulating this specific plant–microbe interaction, our results will foster future proteomic studies aimed at characterizing the very early events of host colonization, thus promoting the development of novel bioassays for pathogen detection in kiwifruit material.

1. Introduction

Bacterial canker of kiwifruit crops (*Actinidia deliciosa* and *A. chinensis*), caused by *Pseudomonas syringae* pv. *actinidiae*, is currently determining relevant economic losses worldwide. Almost contemporarily, a pandemic population of the pathogen has been found in four continents [1]. Thus, Italian and New Zealand institutions provided dedicated

* *Correspondence to:* A. Scaloni, Proteomics and Mass Spectrometry Laboratory, ISPAAM, National Research Council, via Argine 1085, 80147 Naples, Italy. Tel.: +39 081 5966006; fax: +39 081 5965291.
** *Correspondence to:* M. Scortichini, Research Centre for Fruit Crops, Agricultural Research Council (CRA), via di Fioranello 52, 00134 Rome, Italy.
E-mail addresses: andrea.scaloni@ispaam.cnr.it (A. Scaloni), marco.scortichini@entecra.it (M. Scortichini).

1874-3919/$ – see front matter © 2012 Elsevier B.V. All rights reserved.
http://dx.doi.org/10.1016/j.jprot.2012.10.014

funds to the farmers to partly compensate for the severe economic losses. So far, investigations on bacterial canker of kiwifruit mainly focused on the molecular characterization of the pathogen, its country of origin, bioassays for its detection, the cycle of disease, and the climatic factors hampering its multiplication/dispersion in the orchards [2–6]. All the currently cultivated *A. deliciosa* (i.e. Hayward, Green Light, Summerkiwi) and *A. chinensis* (Hort16A, Jintao, Oscar Gold, Soreli) cultivars and their pollinators are susceptible to the pandemic population of *P. s.* pv. *actinidiae*. This bacterium is able to colonize host plants throughout the whole year. Leaf colonization through the stomata seems one of the most important facets of its cycle of disease, either because the pathogen, by inciting extensive leaf spotting, can drastically reduce the host photosynthetic activity or because it can systemically reach the shoot through the leaf veins and petiole [6–8] (Fig. 1A). Once inside the shoot, it can establish an endophytic phase, subsequently leading to canker formation along twig, leader and the main trunk, which is preliminary to evasion toward other plants through the exudates. When the pathogen is inside the plant, it cannot be reached by surface-protecting bactericides (i.e. copper-based compounds).

Nothing is known about the molecular mechanisms underlying the interaction between *P. s.* pv. *actinidiae* and its host plants. Assessment on the protein changes occurring in both organisms during the systemic infection of the shoots is considered important to unveil essential pathways and key effectors assisting pathogen colonization. Proteomic approaches have been already applied to reveal substantial changes in the proteome composition of plant organs infected by pathogenic bacteria and fungi [9–12]. Besides, to elucidate important aspects of plant–microbe interaction [13–17], proteomic studies also contributed to characterize tolerant/resistant cultivars by revealing plant protein species that are selectively represented in the resistant interaction [18–20], or to detect and study bacterial counterparts in apparently healthy hosts that occur during the first phases of the infection process [21–23]. These aspects are particularly important for kiwifruit production upon the current challenge posed by *P. s.* pv. *actinidiae*. Concerning phytopathogenic pseudomonads, the resistance response of *Arabidopsis thaliana* to *P. syringae* pv. *tomato* DC3000 elicited by plant immunomodulators and effectors was evaluated by quantitative gel-based proteomics [24,25]. Later on, the contribution of S-nitrosoglutathione-reductase to the same pathosystem was ascertained by 2D-DIGE [26]. On the other hand, the differences in gene expression patterns during the initial phase of the olive knot disease caused by *P. savastanoi* pv. *savastanoi* were studied by a combined 2-DE/MALDI-TOF peptide mass fingerprint approach [27]. Analogous gel-based proteomic studies were also performed to investigate stress-induced proteins in tomato after challenge with *Ralstonia solanacearum* [28], or in rice and apple-tree during *P. fluorescens* infection [29,30].

In this study, an integrated approach based on differential 2-DE, nanoLC-ESI-LIT-MS/MS and semiquantitative RT-PCR procedures was used to study the interaction between *P. s.* pv. *actinidiae* and *A. chinensis*, during the systemic infection of plant shoots that followed leaf colonization. The current

Fig. 1 – Shoot wilting caused by natural infection of *P. syringae* pv. *actinidiae* on *A. chinensis* (panel A). Shoots of *A. chinensis* cv. Soreli 10 days after the inoculation with *P. syringae* pv. *actinidiae* (panels B and C). This material was further used for proteomic and semiquantitative RT-PCR analysis. Worth noting are the complete wilting of the inoculated leaves and the initial formation of canker along the shoot.

lacking of resistant/tolerant *A. chinensis* germplasm did not allow to compare differences between challenged cultivars and wild-type ones. Identification of down/over-represented protein species in plant and as deriving from bacterium was facilitated by the availability of 132.577 expressed sequence tags (ESTs) for *A. chinensis*, *A. deliciosa*, *A. arguta* and *A. eriantha* [31], the genome sequence of three *P. syringae* pathovars, namely *tomato*, *phaseolicola* and *syringae* [32–34], and the draft genome of three *P. s.* pv. *actinidiae* strains [4]. Differentially represented gene products were characterized as belonging to various functional classes and provided preliminary, but original, insights into the mechanisms underlying the molecular interplay between the yellow-fleshed kiwifruit plant and its currently destructive bacterial pathogen.

2. Materials and methods

2.1. Plant inoculation

Two-year-old, self-rooted, pot-cultivated *A. chinensis* cv. Soreli plants and the pandemic *P. s.* pv. *actinidiae* strain CRA-FRU 8.43 [4] were used for this study. This bacterial strain was originally isolated from *A. chinensis* leaf spot and further characterized [2,35]. Plants were maintained in an aseptic room, with 95% of relative humidity, having natural light and no further fertilization after their receiving from the nursery. The experiment took place in spring (early May). For inoculation, the *P. s.* pv *actinidiae* strain was grown for 48 h on nutrient agar with 3% of sucrose added (NSA), at 25±1 °C. Ten microliters of a bacterial suspension ($1–2\times10^7$ cfu/ml) prepared in sterile 0.85% w/v NaCl were inoculated in the plants chosen for investigation (10 in number). The bacterial suspension was infiltrated at four sites of a young plant leaf, closely to the corresponding vein; two leaves per shoot were inoculated. In parallel, control plants (10 in number) were treated in the same way with sterile saline solution. The inoculated and control plants were randomly distributed in the room, paying attention to avoid their contact. Ten days after inoculation, *A. chinensis* shoots were sampled from infected and control plants for further analyses. This period was chosen since it was demonstrated to coincide with pathogen systemic movement toward plant shoots, determining in some cases initial formation of longitudinal cankers [6]. Leaf and petiole were removed from the shoot samples, which then were divided into three parts, the central one being used for further analyses. From 10 infected (i.e. with leaves wilting) and 10 control plants, 5 biological replicates were generated, respectively, which were then subjected to proteomic analysis (see Supporting Information Fig. S1). Bacterial re-isolation from the infected shoots was performed at the time of sampling as described elsewhere [35].

2.2. Protein sample preparation and quantification

A. chinensis shoot proteins were extracted by using a modified version of the phenol/SDS method optimized for recalcitrant plant tissues [36]. Shoot pieces of about 1 g were thoroughly ground in a pre-cooled mortar with liquid N_2 to obtain a very fine powder; necrotized tissues were not processed. Tissue powder (500 mg) was suspended in 2 ml of ice-cold 500 mM EDTA, 100 mM Tris–HCl pH 8.0, 30% w/v sucrose, 1% w/v polyvinylpolypyrrolidone, 100 mM KCl, 2% w/v SDS, 1 mM phenylmethanesulfonyl fluoride, 5% v/v β-mercaptoethanol, and vortexed for 30 s. Each sample was then added with 2 ml of ice-cold Tris–HCl buffered phenol, pH 8.0, and vortexed thoroughly for 30 s; samples were then centrifuged at 17,000 × g for 5 min, at 4 °C. After centrifugation, the upper phenolic phase was collected and precipitated overnight with 5 vol of cold 100 mM ammonium acetate in methanol, at −20 °C; precipitated proteins were recovered by centrifugation at 17,000 × g for 10 min, at 4 °C. After supernatant removal, the pellet was rinsed three times with 100 mM ammonium acetate in methanol and twice with ice-cold 80% v/v acetone. The pellet was air-dried and resuspended in 2 M thiourea, 7 M urea, 4% w/v CHAPS, 65 mM dithiothreitol (DTT), 10% v/v glycerol, 0.002% w/v bromophenol blue, 0.5% w/v ampholytes pH 3–10 (Bio-Rad, Hercules, CA, USA). Protein concentration was quantified by using the Bio-Rad protein assay kit, which is based on the Bradford method [37], and bovine serum albumin as standard.

2.3. Two-dimension gel electrophoresis

First dimension electrophoresis was performed by using immobilized pH gradient (IPG) strips on an Ettan II IPGphor isoelectric focusing (IEF) system (GE Healthcare). IPG strips (17 cm, 3–10 linear pH gradient) (Bio-Rad) were rehydrated passively with proteins (1 mg) solved in 350 μl of 2 M thiourea, 7 M urea, 4% w/v CHAPS, 65 mM DTT, 10% v/v glycerol, 0.002% w/v bromophenol blue, 0.5% w/v ampholytes pH 3–10, at 20 °C, for 12 h. Afterwards, focusing was performed by applying a constant current of 50 μA per strip, under the same experimental conditions, by using the following program: a liner increase from 0 to 500 V over 1 h, from 500 V to 10,000 V over 5 h, and then held at 10,000 V for a total of 100 kVh. After IEF, proteins were reduced by incubating the IPG strips with equilibration buffer (50 mM Tris–HCl pH 8.8, 6 M urea, 2% w/v SDS, 30% v/v glycerol, 0.002% w/v bromophenol blue) containing 1% w/v DTT, for 10 min, and alkylated with 2.5% w/v iodoacetamide in equilibration buffer, for 10 min. IPG strips were then transferred onto 12% SDS-PAGE gels for the second dimension electrophoresis, which was performed in a Protean II (Bio-Rad) unit, using 25 mM Tris pH 8.3, 0.2 M glycine, 35 mM SDS as running buffer. Samples were run using the following program: 25 mA for 20 min, 40 mA for 80 min, 50 mA for 140 min, 60 mA for 100 min, and 70 mA for 30 min. Gels were stained with colloidal Coomassie Blue R-350 (GE Healthcare) and then de-stained according to the manufacturer's recommendations. To account for experimental electrophoretic variations, triplicate gels for each biological sample were analyzed in parallel. Gel images were acquired by using an Image Scanner III flatbed scanner (GE Healthcare). Molecular mass and p*I* values were estimated by running a control sample together with protein standards (Bio-Rad).

2.4. Gel image analysis

Digitized images of Coomassie-stained gels were analyzed by using the ImageMaster™ 2D Platinum software (GE Healthcare), which allowed spot detection, landmarks identification, aligning/matching of spots within gels, quantification of matched spots

and their analysis. Manual inspection of the spots was performed to verify the accuracy of the automatic gel matching; any error in the automatic procedure was manually corrected prior to the final data analysis. The spot volume was used as the analysis parameter for quantifying protein expression. The protein spot volume was normalized to the spot volume of the entire gel (i.e., of all the protein spots). Fold changes in protein spot levels were calculated between spot volumes in the infected group relative to that in the control one. Statistically significant changes in protein abundance were determined by using two sequential data analysis criteria. First, a protein spot had to be present in all gels for each sample to be included in the analysis. Next, statistically significant quantitative changes were determined by using the distribution of fold change values in the data. Spots were determined to be statistically significant if the difference between the average intensity of a specific protein spot in the infected and control plants (three technical replicates of five biological samples) was greater than one standard deviation of the spot intensities for both groups. An absolute two-fold change in normalized spot densities was then considered as indicative of a significant quantitative variation. For statistical analysis, data were processed by using the Statistical Package for Social Science software (IBM Spss Statistics) through missing value imputation via K-nearest neighbors analysis, followed by log-transformation of the imputed data and comparison of control and treated values to evaluate corresponding variance (ANOVA), with a non-linear mixed-effects model. P values <0.05 were considered to be significant.

2.5. *In-gel digestion and mass spectrometry*

Spots were manually excised from gels, alkylated and digested with trypsin, as previously reported [38,39]. Digest aliquots were removed and subjected to a desalting/concentration step on μZipTipC18 (Millipore, Bedford, MA, USA) using acetonitrile as eluent before nanoLC-ESI-LIT-MS/MS analysis. Peptide mixtures were analyzed by nanoLC-ESI-LIT-MS/MS using a LTQ XL mass spectrometer (Thermo) equipped with Proxeon nanospray source connected to an Easy-nanoLC (Proxeon) [38,39]. Peptide mixtures were separated on an Easy C_{18} column (100×0.075 mm, 3 μm) (Proxeon) using a linear gradient of 0.1% v/v formic acid, acetonitrile (solvent B) in 0.1% v/v formic acid (solvent A) from 5 to 35% over 15 min, and from 35 to 95%, over 2 min, at a flow rate of 300 nl/min. Spectra were acquired in the range of m/z 300–1800. Acquisition was controlled by a data-dependent product ion scanning procedure over the three most abundant ions, enabling dynamic exclusion (repeat count 2 and exclusion duration 1 min). The mass isolation window and collision energy were set to m/z 3 and 35%, respectively.

2.6. *Protein identification*

Raw data files from nLC-ESI-LIT-MS/MS experiments were searched by MASCOT search engine (version 2.2.06, Matrix Science, UK) against two updated databases from NCBI (2011/10/27), containing available *Actinidia* EST and *Pseudomonas* protein sequences, respectively. Database searching was performed by using a mass tolerance value of 2 Da for precursor ion and 0.8 Da for MS/MS fragments, trypsin as proteolytic enzyme, a missed cleavages maximum value of 2, and Cys carbamidomethylation and Met oxidation as fixed and variable modifications, respectively. Candidates with more than 2 assigned peptides with an individual MASCOT significance threshold P value <0.05 were considered confidently identified. Definitive peptide assignment was always associated to manual spectral visualization and verification. Where appropriate, protein identification was further evaluated by the comparison with their calculated mass and pI values, using the experimental values obtained from 2-DE. Identified *Actinidia* spp. EST entries were associated with specific enzymes/proteins from other plant species by using the BLAST program (http://blast.ncbi.nlm.nih.gov/Blast.cgi).

2.7. *Semiquantitative RT-PCR analysis*

Ten days after *A. chinensis* inoculation, RNA was isolated from infected and control shoots by using the RNeasy plant mini kit (Qiagen, Hilden, Germany), according to the manufacturer's instructions. Three biological replicates were analyzed for different infected or control plants, respectively. RNA concentration was assessed by UV/visible spectroscopy, while its structural integrity was checked on a non-denaturing agarose gel, followed by ethidium bromide staining.

First-strand cDNA was synthesized from 3 μg of total RNA using oligo$(dT)_{20}$ primers using the ThermoScript RT-PCR System (Invitrogen Life Technologies, Carlsbad, CA, USA), according to manufacturer's recommendations. For semiquantitative RT-PCR analysis, 2 μl of cDNA was amplified with 1 unit of Platinum® Taq High Fidelity (Invitrogen) in 1× PCR buffer containing 2 mM $MgCl_2$, in the presence of 200 μM of each dNTP and one gene-specific primer pair (0.4 μM of each oligonucleotide); final reaction volume: 50 μl. Primer oligonucleotide pairs of oxygen-evolving enhancer protein 1, chlorophyll a-b binding protein 3C, actinidain, 23.6 kDa heat shock protein and glutathione S-transferase genes were designed by using Primer3 software [40] (Table 1). Glucose-6-phosphate dehydrogenase (EF063567.1) was used as housekeeping gene. To detect differences in cDNA expression levels for each sample set, a variable number of amplification cycles (20–25 depending on gene templates) was tested (Table 1). PCR reaction conditions were: 94 °C for 3 min, followed by n amplification cycles (optimized for each gene) at 94 °C for 30 s, the appropriate annealing

Table 1 – Genes, primers and different parameters used for semiquantitative RT-PCR experiments.

Gene name	Primer sequence 5′ to 3′ (forward/reverse)	T annealing (°C)	n° cycles
G6PD1	GGGATTTTTGCAATCCAATG CCCCAGAGTCATAGGAACCA	55	25
PBSO	TGCTCTTGGTGACACTGAGG CGGTAAACCAGAGAGCTTCG	60	24
CAB3C	CCATCCTACTTGACGGGAGA ACCATACAGCCTCACCGAAC	60	22
ACTN	CTGCAACAGCGGTTTAATGA GCATCAATGCCAACACTCAC	55	23
HSP23.6	ATGTGGGTTCTGTGGAAAGC TCACATTCCACCCTCTCCTC	58	25
GST	ACATTGATGAGGCCTGGAAG CCCCAAGGGCTTTTTCTAAC	55	24

temperature for 1 min, 72 °C for 2 min, and a final extension of 7 min at 72 °C. Amplified products were resolved on 1.8% agarose gels containing ethidium bromide and visualized by using a GelDoc Imaging system (Bio-Rad, Hercules, CA). Experiments were done with three independent biological replicates, each of them with three technical replicates.

3. Results and discussion

3.1. *A. chinensis* shoot proteome after inoculation with *P. s. pv. actinidiae*

Initial wilting of the *A. chinensis* leaves inoculated with the pandemic *P. s.* pv. *actinidiae* strain CRA-FRU 8.43 appeared about 3–4 days after bacterial challenge. Ten days after inoculation, leaves were completely wilted and the initial formation of a longitudinal canker along the shoot was evident (Fig. 1B and C). Pathogen started the systemic shoot colonization 4–5 days after leaf inoculation. At this time, we re-isolated bacterial colonies at the insertion of the petiole on the shoot, which were further identified as the inoculated *P. s.* pv. *actinidiae* strain [2,35]. Ten days after the leaf inoculation, bacterial density in the shoot varied from 1×10^7 to $1–3\times10^8$ cfu/g of tissue. At this time, protein extracts from the mid-shoot of inoculated *A. chinensis* plants were prepared, analysed in 2-DE experiments and compared to that from control plants. Initial protein concentration within extracts was 3.16±0.16 and 2.55±0.12 mg/g shoot dry weight for inoculated and control samples, respectively. Gel-based proteomic experiments were accomplished by performing IEF within the p*I* range 3–10 and SDS-PAGE within the mass range 10–100 kDa. Spots representing proteins with extreme p*I* or Mr values were not clearly resolved. Resulting average proteomic maps showed 544±21 (inoculated) and 518±13 (control) spots, with a degree of similarity for the inoculated compared to healthy plants of 95.2±2.1%. We assessed the degree of technical variation inherent to the 2D process by using the coefficient of variation (CV) in biological and technical replicates for all spots matched in five master gels. For the control samples investigated, the average CV was 18% and 19% in biological and technical replicates, respectively; for the inoculated samples, it was 16% and 21% in biological and technical replicates, respectively. Quantitative evaluation of protein spots visible in all replicate gels corresponding to the same experimental condition was then accomplished to evaluate differential protein representation following bacterial attack. Image analysis of proteomic maps identified statistically significant variations between the two conditions. Fig. 2 shows a representative image of a colloidal Coomassie-stained gel corresponding to control (panel A) and infected (panel B) plant state, which were both used for spot picking. One hundred seventeen protein spots presented significant relative fold change variations ($P<0.05$). In particular, 31 spots showed quantitative changes, while 55 and 31 ones uniquely occurred in inoculated or control plants, respectively. Examples of the first category are shown in Fig. 3. All corresponding gel portions were excised from gel, trypsinized and characterized by nanoLC-ESI-LIT-MS/MS (Supporting Information Table S1). The presence of multiple spots identified as the same protein species, occurring with the horizontal train's aspect typical of glycosylated/phosphorylated polypeptides, led to the final recognition of 88 protein entries that were associated with specific components from other plant species, following their BLAST analysis with respect to the *Viridiplantae* database (Table 2). In general, most of the identified *A. chinensis* protein species showed experimental p*I* and Mr values in good agreement with the theoretical ones calculated for the corresponding counterparts from other plant species. On the other hand, a unique spot was identified as a *Pseudomonas* gene product, namely outer membrane porin F.

For protein categorization, the methods of Bevan et al. [41] was followed, which allowed polypeptide grouping into 10 functional classes (Table 2). Disease/defence protein species were the most represented group, followed by gene products involved in energy regulation, metabolism, protein destination and storage, transport, unclassified, cell structure, protein synthesis, cell growth/division and secondary metabolism (Fig. 4). In general, this distribution resembled that already described for other pathosystems [10,11], but also highlighted peculiarities associated with the plant organ here investigated.

In order to verify transcriptional regulation of some of the identified proteins reported in Table 2, we detected their transcripts by RT-PCR. Some representative examples of the different functional classes reported above were chosen to this purpose; their selection was arbitrary. As shown in Fig. 5, all tested genes, i.e. oxygen-evolving enhancer protein 1 (*PSBO*), chlorophyll a-b binding protein 3C (*CAB3C*), actinidain (*ACTN*), 23.6 kDa heat shock protein (*HSP23.6*) and glutathione S-transferase (*GST*), showed a good quantitative correlation between transcript and protein levels at the experimental time points/interactions chosen for analysis. These experiments suggested that expression of most deregulated plant genes after *P. s.* pv. *actinidiae* infection is controlled at transcriptional level.

3.2. Plant proteins involved in defence mechanisms

Protein species that were over-represented in *A. chinensis* shoots following *P. s.* pv. *actinidiae* infection included members of different plant defence categories, such as pathogenesis-related (PR) polypeptides or components involved in basal protection, oxidative stress, heat shock, and related transport and signalling processes (Table 2), suggesting that host response to bacterial challenge involves independent molecular pathways [10,11]. Within the basal defence proteins, serpin ZX and hypersensitivity induced response (HIR) protein 1 species (spots 74, 75 and 83) were identified as augmented after bacterial infection. Serpins are molecular inhibitors eliciting a defensive action against the proteases present within phytophagous insect gut or secreted by microorganisms, thus determining a reduction in the availability of amino acids necessary for their growth [42]; other protease inhibitors are over-represented in various pathosystems [43]. On the other hand, HIR proteins contribute to the development of hypersensitivity reaction in leaves attacked by pathogens [44] and have already been ascertained as augmented in the rice/*Xanthomonas oryzae* pathosystem [45].

Among PR gene products only detected in inoculated *A. chinensis* shoots, worth-mentioning are PR-1, glucan endo1,3-β-glucosidase, endochitinase B, chitinase class IV, thaumatin-like precursor, Bet v1-related allergen and PR-4 species (spot 98, 80, 82, 86, 90, 92–94, 96, and 99), which are type-members of plant PR

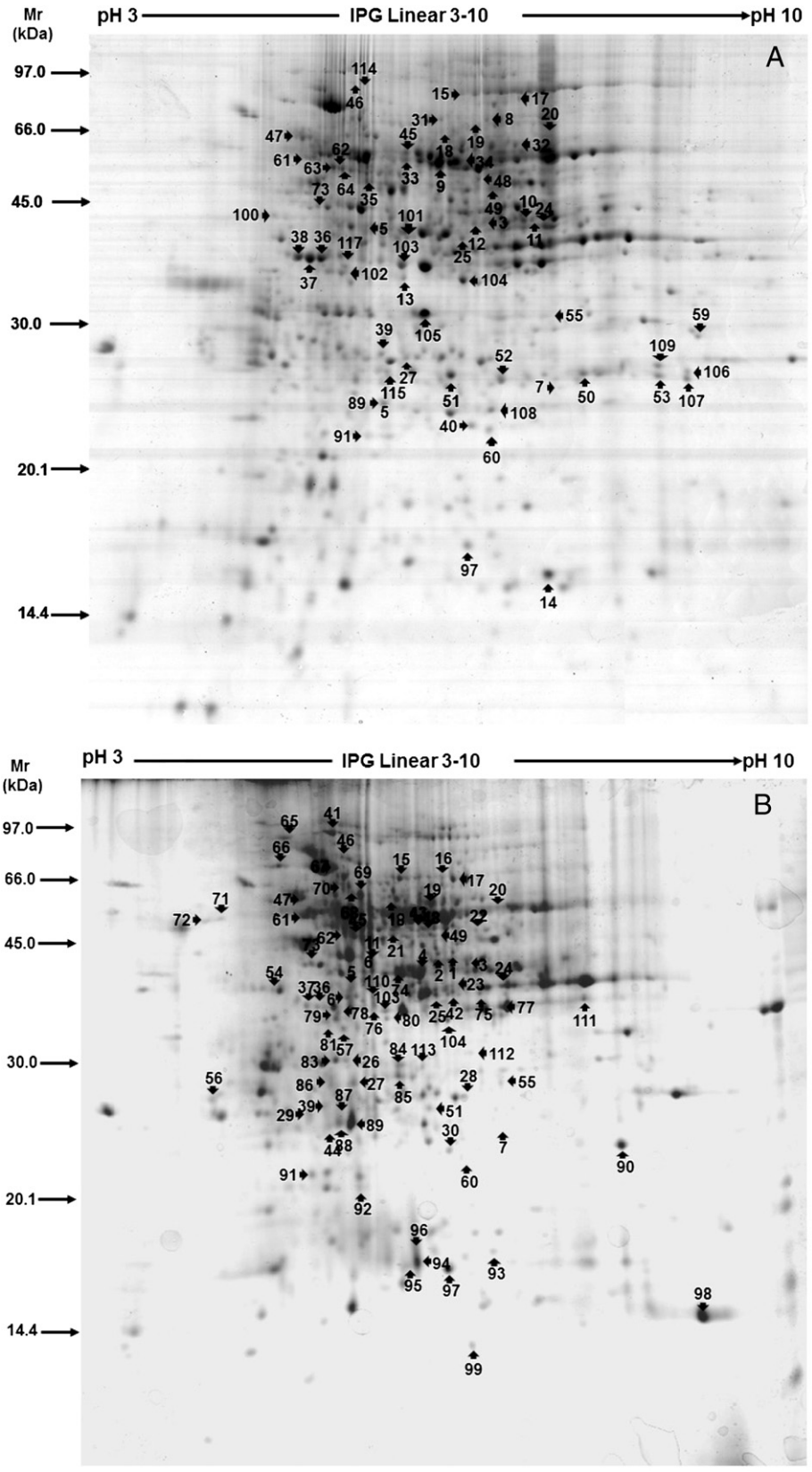

Fig. 2 – Representative 2-DE gels of total protein extracts from shoots of control (panel A) and *P. syringae* pv. *actinidiae*-inoculated *A. chinensis* cv. Soreli (panel B). Protein separation was based on IEF using linear gel strips in the range of pH 3–10 and on SDS-PAGE in the size range 10–100 kDa. Gels were stained with colloidal Coomassie Blue R-350. Spot numbering refers to Table 2 and shows protein identification as obtained by nLC-ESI-LIT-MS/MS analysis.

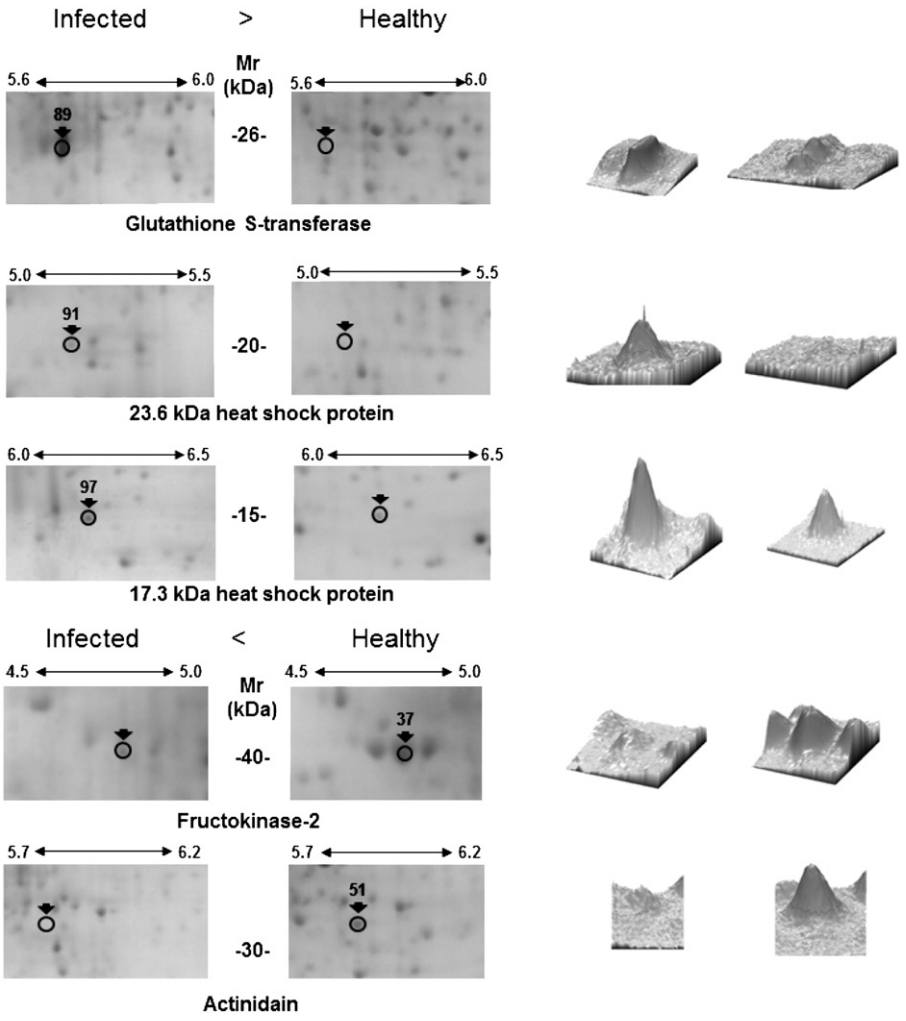

Fig. 3 – Representative cropped gel regions comprising some statistically significant changes in the proteomic repertoire of *P. syringae* pv. *actinidiae*-infected and non-infected *A. chinensis* cv. Soreli shoots. Corresponding normalized spot volume of each protein spot in healthy and infected tissues is reported in Table 2, together with spot numbering.

families 1, 2, 3, 4, 5 and 10, already associated with bacterial infection in other plants [10,16,18,20,25,26,43]. In particular, PR-1 is considered as a biomarker of the enhanced defensive state incited by pathogen-induced systemic acquired resistance, even though its precise activity still remains unclear [46]. Several β-1,3-glucanases degrading polysaccharides are constitutively over-represented during bacterial infection [10,26,43,46,47]; in the tomato/*Cladosporium fulvum* pathosystem, their highest concentration was measured at days 4–8 and 8–12 after inoculation with an avirulent and a virulent pathogen, respectively [48]. Chitinases are either supposed to confer a broad resistance to bacterial/fungal pathogens and to release pathogen-borne elicitors further inducing host defence reactions [10,49,50]. Thaumatin-like protein expression is induced in tissues with prominent vascularization by phytohormones related to plant defence (i.e. salicylic acid and jasmonic acid) [16,51,52]; this protein is supposed to play a role in promoting pore formation in the bacterial membrane [53]. Finally, PR-10 protein species are widespread in plants [46,54] and are known to be over-represented upon pathogen infection [55,56].

After bacterial challenge, we also observed an augmented concentration of 17.3 kDa heat shock protein (HSP) (spots 95 and 97), 23.6 kDa HSP (spot 91), CPN60 (spots 68, 69 and 70), endoplasmin homolog (spot 65) and 70 kDa HSP (spot 66 and 67) species, confirming recent studies on other pathosystems [10,16]. Proteomic data on 23.6 kDa HSP were also confirmed at transcriptional level (Fig. 5). HSPs are essential for polypeptide folding/assembling but have also been associated with plant basal resistance to pathogen attack [10,57]. In particular, HSP70 is involved in the complex assembly of chloroplast-resident defence factors [57]. Recently, its induction in plants has been recognized in the early events associated with *P. syringae* pathovars infection [58]. In this case, bacterial effector protein HopI1, also present in *P. s.* pv. *actinidiae* [4], should bind to plant HSP70 and recruit it to the chloroplast, suppressing host defences [58]. Our results confirmed that HSP70 is also actively involved in the compatible *A. chinensis*/*P. s.* pv. *actinidiae* interaction. Increasing evidences indicate that plants also use the ubiquitin/26S proteasome pathway in their immune response to bacterial/fungal invasion [59,60]. Accordingly, a number of proteasome

Table 2 – Differentially represented protein species present in *A. chinensis* cv. Soreli shoots following inoculation with *P. syringae* pv. *actinidiae*. Protein species are classified according to functional categories. Spots identified by using nLC-ESI-LIT-MS/MS are reported. Spot number, protein name, kiwi EST accession, SwissProt entry with the highest sequence identity after BLAST analysis, corresponding organism, sequence identity between EST and SwissProt entries, sequence coverage percentage, number of non-redundant peptides identified, theoretical and experimental *Mr* and *pI* values are listed. Plus and minus refer to protein species present or absent in a unique condition. For over/down-represented proteins, the corresponding normalized spot volume value is reported.

Spot	Protein name	Kiwi EST accession	Homologous protein – SwissProt code (sequence identity %)	Organism	Sequence coverage % (unique peptides)	Theor. *Mr*/*pI*	Exp. *Mr*/*pI*	Normalized spot volume	
								Control	Inoculated
Metabolism									
1	Alcohol dehydrogenase	195264893	P14675 (88)	*Solanum tuberosum*	12 (3)	41/5.92	46/6.32	–	+
2	Alcohol dehydrogenase	195264893	P14675 (88)	*Solanum tuberosum*	21 (6)	41/5.92	46/6.15	–	+
3	Alcohol dehydrogenase	195264893	P14675 (88)	*Solanum tuberosum*	14 (4)	41/5.92	43/6.50	0.05±0.01	0.22±0.05
4	Glutamine synthetase cytosolic isozyme 1	195204429	P51118 (95)	*Vitis vinifera*	14 (5)	39/5.79	42/6.03	–	+
5	Adenosine kinase 2	195285550	Q9LZG0 (85)	*Arabidopsis thaliana*	18 (4)	38/5.14	36/5.32	0.06±0.02	0.32±0.09
6	Adenosine kinase 2	195198228	Q9LZG0 (83)	*Arabidopsis thaliana*	8 (2)	38/5.14	35/5.29	–	+
7	Fumarylacetoacetate hydrolase	195226447	B9RT83 (91)	*Ricinus communis*	23 (3)	24/6.52	25/6.26	0.04±0.01	0.23±0.06
8	Methylenetetrahydrofolate reductase	195203290	Q75HE6 (85)	*Oryza sativa*	10 (4)	66/5.38	68/6.00	+	–
9	Adenosylhomocysteinase	195305570	P50246 (93)	*Medicago sativa*	33 (11)	53/5.69	58/5.71	+	–
10	Glutamate dehydrogenase B	195318047	A7YVW3 (97)	*Actinidia chinensis*	24 (7)	44/6.32	45/6.02	+	–
11	Glutamate dehydrogenase A	195194844	A7YVW4 (99)	*Actinidia chinensis*	23 (9)	45/6.28	45/6.16	+	–
12	Patatin-like protein 3	195286287	Q9FZ08 (70)	*Nicotiana tabacum*	13 (3)	45/7.70	43/5.91	+	–
13	Thiosulfate sulfurtransferase	195241029	B9RHZ9 (90)	*Ricinus communis*	14 (3)	42/6.57	37/5.60	+	–
14	Nucleoside diphosphate kinase 1	195218902	Q56E62 (89)	*Nicotiana tabacum*	18 (2)	16/6.30	11/6.79	+	–
Energy									
15	Succinate dehydrogenase [ubiquinone] flavoprotein subunit 1	195320293	Q82663 (95)	*Arabidopsis thaliana*	15 (6)	66/5.58	75/5.85	0.09±0.03	0.35±0.12
16	NADP-dependent malic enzyme	195213639	P51615 (91)	*Vitis vinifera*	13 (6)	65/6.09	76/6.20	–	+
17	NADP-dependent malic enzyme	195213639	P51615 (91)	*Vitis vinifera*	17 (9)	65/6.09	74/6.33	0.08±0.01	0.24±0.05
18	ATP synthase subunit α	195320376	Q01915 (97)	*Glycine max*	7 (4)	55/6.23	66/5.82	0.04±0.01	0.23±0.04
19	NAD-dependent malic enzyme 59 kDa isoform	195317860	P37225 (85)	*Solanum tuberosum*	11 (4)	64/5.48	62/5.85	0.08±0.03	0.40±0.06
20	Aldehyde dehydrogenase	195197050	Q1AFF6 (81)	*Vitis pseudoreticulata*	7 (3)	58/8.04	63/6.92	0.04±0.01	0.25±0.05
21	Enolase	195271344	D7T227 (92)	*Vitis vinifera*	25 (9)	48/6.17	54/5.78	–	+
22	6-phosphogluconate dehydrogenase	195276481	O22111 (91)	*Glycine max*	17 (6)	56/5.55	54/6.60	–	+
23	Isocitrate dehydrogenase	195298237	O65852 (83)	*Nicotiana tabacum*	14 (6)	36/6.08	37/6.32	–	+
24	Malate dehydrogenase	195249343	P83373 (88)	*Fragaria* x *ananassa*	21 (6)	33/6.34	37/6.96	0.05±0.02	0.25±0.09
25	UDP-glucose 4-epimerase GEPI48	195217967	O65781 (84)	*Cyamopsis tetragonoloba*	14 (4)	38/6.72	36/6.13	0.04±0.01	0.21±0.07
26	Oxygen-evolving enhancer protein 1	195247166	P23322 (95)	*Solanum lycopersicum*	36 (9)	27/5.10	29/5.28	–	+
27	6-phosphogluconolactonase 5	195216181	E0CVA1 (81)	*Vitis vinifera*	8 (2)	28/5.66	27/5.33	0.06±0.01	0.41±0.08
28	Triosephosphate isomerase	195201084	D1LWT8 (94)	*Dimocarpus longan*	21 (4)	27/6.13	26/6.44	–	+
29	Chlorophyll a-b binding protein 3C	195258845	P07369 (87)	*Solanum lycopersicum*	28 (4)	25/5.12	25/5.02	–	+
30	Oxygen-evolving enhancer protein 2	195210869	P16059 (80)	*Pisum sativum*	44 (8)	20/5.52	22/6.25	–	+
31	Succinate dehydrogenase [ubiquinone] flavoprotein subunit 1	195237595	O82663 (92)	*Arabidopsis thaliana*	4 (2)	66/5.58	56/4.97	+	–
32	Plastocyanin	195238502	P00289 (75)	*Spinacia oleracea*	18 (2)	17/5.32	63/6.26	0.21±0.02	0.07±0.01
33	Enolase 2	195271344	Q9LEI9 (91)	*Hevea brasiliensis*	19 (6)	48/5.92	60/5.60	+	–

Table 2 (*continued*)

Spot	Protein name	Kiwi EST accession	Homologous protein – SwissProt code (sequence identity %)	Organism	Sequence coverage % (unique peptides)	Theor. Mr/pI	Exp. Mr/pI	Normalized spot volume	
								Control	Inoculated
34	Mitochondrial-processing peptidase subunit β	195252044	F6H5N5 (94)	*Vitis vinifera*	27 (16)	56/5.95	58/5.83	+	–
35	Mitochondrial-processing peptidase	195313199	D7TBD9 (86)	*Vitis vinifera*	16 (6)	55/5.71	53/5.43	+	–
36	Fructokinase-2	195208447	Q7XJ81 (88)	*Solanum habrochaites*	50 (13)	35/5.91	41/4.87	0.36±0.02	0.10±0.01
37	Fructokinase-2	195208447	Q7XJ81 (88)	*Solanum habrochaites*	52 (15)	35/5.91	40/4.81	0.70±0.03	0.24±0.03
38	Fructokinase-2	195208447	Q7XJ81 (88)	*Solanum habrochaites*	34 (9)	35/5.91	41/4.75	+	–
39	Triosephosphate isomerase	195242577	A9P7V6 (90)	*Popolus trichocarpa*	22 (4)	27/6.45	30/5.51	0.21±0.05	0.05±0.01
40	Oxygen-evolving enhancer protein 2	195210869	P16059 (80)	*Pisum sativum*	48 (6)	20/5.52	25/5.90	+	–
Cell growth/division									
41	Cell division cycle protein 48 homolog	195217080	Q96372 (91)	*Capsicum annuum*	9 (6)	89/5.07	76/5.20	–	+
42	Histone H4	195282042	F2E7L1 (19)	*Hordeum vulgare distichum*	4 (2)	50/9.97	36/6.32	–	+
Protein synthesis									
43	Eukaryotic initiation factor 4A-11	195262580	Q40465 (95)	*Nicotiana tabacum*	10 (5)	47/5.38	54/6.00	–	+
44	60S ribosomal protein L9	195210870	P30707 (87)	*Pisum sativum*	15 (3)	22/9.32	23/5.08	–	+
45	Eukaryotic initiation factor 4A-15	195284580	Q40468 (99)	*Nicotiana tabacum*	25 (10)	47/5.38	52/5.34	0.05±0.01	0.52±0.03
Protein destination and storage									
46	Uncharacterized protein	195238889	F6H1E0 (85)	*Vitis vinifera*	6 (3)	81/6.10	80/5.26	0.05±0.02	0.27±0.05
47	Protein disulfide isomerase	195194301	Q43116 (77)	*Ricinus communis*	14 (4)	53/4.91	66/4.99	0.02±0.01	0.24±0.06
48	Uncharacterized protein	195214386	D7SRG7 (89)	*Vitis vinifera*	18 (5)	43/6.40	52/6.09	0.08±0.03	0.28±0.08
49	Predicted protein	195195976	A9PF64 (87)	*Populus trichocarpa*	8 (2)	44/6.58	52/6.13	0.05±0.02	0.28±0.08
50	Actinidain	195214977	P00785 (68)	*Actinidia chinensis*	10 (2)	27/4.37	29/6.90	+	–
51	Actinidain	195214977	P00785 (68)	*Actinidia chinensis*	11 (3)	27/4.37	26/6.00	0.36±0.03	0.10±0.01
52	Actinidain	195213415	P00785 (63)	*Actinidia chinensis*	37 (6)	27/4.37	28/6.05	+	–
53	Actinidain	195213415	P00785 (63)	*Actinidia chinensis*	18 (5)	27/4.37	28/8.88	+	–
Transporters									
54	Outer membrane porin F	330967341	P22263 (98)	*Pseudomonas syringae* pv. *syringae*	30 (8)	34/4.60	34/4.75	–	+
55	GTP-binding nuclear protein Ran1	195289812	P38546 (100)	*Solanum lycopersicum*	11 (2)	25/6.24	27/6.94	0.07±0.02	0.26±0.09
56	Nascent polypeptide-associated complex subunit alpha-like	195202150	D7UCZ6 (91)	*Vitis vinifera*	44 (5)	22/4.32	26/4.45	–	+
57	α-soluble NSF attachment protein	195215525	P93798 (78)	*Vitis vinifera*	19(4)	32/4.85	32/5.26	–	+
58	α-soluble NSF attachment protein	195215525	P93798 (78)	*Vitis vinifera*	29(6)	32/4.85	38/5.10	+	–
59	Mitochondrial outer membrane protein porin of 36 kDa	195230934	P42056 (82)	*Solanum tuberosum*	21 (7)	29/7.91	31/9.50	+	–
60	Apolipoprotein d	195310468	B9SBY6 (81)	*Ricinus communis*	19(3)	22/6.33	25/5.99	0.22±0.07	0.06±0.03
Cell structure									
61	Tubulin β-2 chain	195232691	Q8H7U1 (98)	*Oryza sativa*	21 (8)	50/4.72	59/5.01	0.03±0.01	0.24±0.05
62	Tubulin α-3/α-5 chain	195264821	P20363 (98)	*Arabidopsis thaliana*	29 (10)	50/4.95	54/5.29	0.05±0.02	0.28±0.06
63	Tubulin α chain	195252777	P33629 (99)	*Prunus dulcis*	32 (10)	50/4.92	57/4.93	+	–

(*continued on next page*)

Table 2 (*continued*)

Spot	Protein name	Kiwi EST accession	Homologous protein – SwissProt code (sequence identity %)	Organism	Sequence coverage % (unique peptides)	Theor. Mr/pI	Exp. Mr/pI	Normalized spot volume	
								Control	Inoculated
64	Tubulin α chain	195252777	P33629 (99)	*Prunus dulcis*	26 (9)	50/4.92	56/4.97	+	–
Disease/defence									
65	Endoplasmin homolog	195284178	P35016 (90)	*Catharanthus roseus*	12 (10)	91/4.83	76/4.87	–	+
66	Stromal 70 kDa heat shock-related protein	195284640	Q02028 (92)	*Pisum sativum*	4 (2)	68/4.83	80/4.84	–	+
67	Heat shock cognate 70 kDa protein 1	195241024	A5C0Z3 (93)	*Vitis vinifera*	6 (4)	71/5.17	83/5.22	–	+
68	Chaperonin CPN60	195215108	P29197 (90)	*Arabidopsis thaliana*	20 (8)	57/5.19	71/5.31	–	+
69	Chaperonin CPN60	195302062	P29197 (89)	*Arabidopsis thaliana*	6 (3)	57/5.19	66/5.40	–	+
70	Chaperonin CPN60	195263243	P29197 (90)	*Arabidopsis thaliana*	18 (7)	57/5.19	69/5.27	–	+
71	26S proteasome non-ATPase regulatory subunit 4	195295813	I1LI24 (93)	*Glycine max*	19 (6)	43/4.58	59/4.51	–	+
72	26S proteasome non-ATPase regulatory subunit 4	195195161	I1LI24 (93)	*Glycine max*	8 (2)	43/4.58	57/4.41	–	+
73	Polyphenol oxidase	195246920	A5BPY3 (71)	*Vitis vinifera*	8 (3)	67/6.37	43/5.04	0.08±0.01	0.28±0.02
74	Serpin ZX	195252434	Q8GT65 (80)	*Citrus paradisi*	17 (4)	42/6.04	42/5.81	–	+
75	Hypersensitive-induced response protein 1	195264653	Q9FM19 (90)	*Arabidopsis thaliana*	14 (4)	31/5.29	36/6.65	–	+
76	Isoflavone reductase homolog P3	195200739	B2WSN1 (86)	*Petunia hybrida*	10 (2)	34/5.51	34/5.62	–	+
77	Annexin	195232846	B9RGC9 (67)	*Ricinus communis*	30(10)	36/6.04	34/6.95	–	+
78	Proteasome subunit α type-1-A	195245555	P34066 (90)	*Arabidopsis thaliana*	22 (4)	30/4.99	34/5.22	–	+
79	Proteasome subunit α type-1-A	195245555	P34066 (90)	*Arabidopsis thaliana*	28 (8)	30/4.99	33/5.20	–	+
80	Glucan endo 1,3-β-glucosidase	195285421	P36401 (63)	*Nicotiana tabacum*	8 (2)	34/5.23	33/5.73	–	+
81	Proteasome subunit α type-1-A	195287284	P34066 (91)	*Arabidopsis thaliana*	14 (4)	30/4.99	33/5.15	–	+
82	Endochitinase B	195212155	P24091 (85)	*Nicotiana tabacum*	41 (7)	31/8.31	31/8.32	–	+
83	Hypersensitive-induced response protein 1	195264653	Q9FM19 (90)	*Arabidopsis thaliana*	44 (11)	31/5.29	29/5.20	–	+
84	L-ascorbate peroxidase	195249969	Q1W3C7 (92)	*Camelia sinensis*	39 (9)	27/5.87	28/5.83	–	+
85	L-ascorbate peroxidase	195249969	Q1W3C7 (92)	*Camelia sinensis*	40 (7)	27/5.87	28/5.83	–	+
86	Class IV chitinase	195197069	G8IEM3 (100)	*Actinidia chinensis*	25 (5)	29/5.59	27/5.17	–	+
87	Glutathione S-transferase	195312193	F6HR78 (70)	*Vitis vinifera*	11 (2)	25/5.55	24/5.22	–	+
88	Proteasome subunit β type-6	195196727	Q8LD27 (88)	*Arabidopsis thaliana*	18 (3)	24/5.54	24/5.19	–	+
89	Glutathione S-transferase	195274111	Q03666 (75)	*Nicotiana tabacum*	17(6)	26/5.65	24/5.31	0.28±0.02	1.51±0.07
90	Thaumatin-like protein precursor	195241346	P81370 (95)	*Actinidia deliciosa*	43 (9)	22/7.91	22/8.63	–	+
91	23.6 kDa heat shock protein	195283457	H6TB40 (67)	*Citrullus lanatus*	20 (3)	23/5.06	20/5.03	0.08±0.01	0.33±0.05
92	Bet v1-related allergen	195194362	D1YSM4 (95)	*Actinidia chinensis*	15 (2)	17/5.82	19/5.37	–	+
93	Bet v1-related allergen	195194362	D1YSM4 (95)	*Actinidia chinensis*	16 (2)	17/5.82	16/6.23	–	+
94	Bet v1-related allergen	195198226	D1YSM4 (99)	*Actinidia chinensis*	72 (15)	17/5.82	16/5.74	–	+
95	17.3 kDa class II heat shock protein	195245822	O82013 (78)	*Solanum peruvianum*	32 (4)	17/6.32	16/5.75	–	+
96	Bet v1-related allergen	195198226	D1YSM4 (99)	*Actinidia chinensis*	59 (7)	17/5.82	16/5.00	–	+
97	17.3 kDa class II heat shock protein	195245822	O82013 (78)	*Solanum peruvianum*	46 (6)	17/4.87	15/6.23	0.14±0.09	0.66±0.11
98	Pathogenesis-related protein PR-1 type	195235158	E2GEU6 (70)	*Vitis vinifera*	68 (6)	17/8.12	13/9.66	–	+
99	Pathogenesis-related protein 4	195220941	G9JVT0 (78)	*Vitis pseudoreticulata*	24 (3)	15/8.12	12/6.52	–	+
100	Polyphenol oxidase	195246920	A5BPY3 (71)	*Vitis vinifera*	10 (3)	67/6.37	45/4.62	+	–
101	Polyphenol oxidase	195249443	A5BPY3 (64)	*Vitis vinifera*	12 (7)	67/6.37	42/5.61	+	–

Table 2 (*continued*)

Spot	Protein name	Kiwi EST accession	Homologous protein – SwissProt code (sequence identity %)	Organism	Sequence coverage % (unique peptides)	Theor. *Mr*/*pI*	Exp. *Mr*/*pI*	Normalized spot volume	
								Control	Inoculated
102	Proteasome subunit α type-1-A	195287284	P34066 (91)	*Arabidopsis thaliana*	40 (10)	30/4.99	39/4.98	+	–
103	Isoflavone reductase homolog P3	195200739	B2WSN1 (86)	*Petunia hybrida*	30 (9)	34/5.51	39/5.60	0.87±0.08	0.10±0.01
104	Annexin	195274134	B9HFG8 (82)	*Popolus trichocarpa*	46 (13)	36/6.34	37/5.87	0.39±0.05	0.10±0.02
105	Abscisic acid stress ripening protein	195192941	D4Q9L8 (44)	*Prunus mume*	16 (3)	22/5.97	32/5.70	+	–
106	Proteasome subunit β type	195209889	D7SKV3 (89)	*Vitis vinifera*	19 (4)	25/6.44	28/9.38	+	–
107	Proteasome subunit β type	195202003	D7SKV3 (89)	*Vitis vinifera*	37 (7)	25/6.44	28/9.36	+	–
108	Minor allergen Alt a	195321240	B9T876 (92)	*Ricinus communis*	9 (2)	22/6.10	26/6.00	+	–
109	Osmotin-like protein	195196068	Q41350 (72)	*Oryza sativa*	17 (3)	21/7.94	29/8.87	+	–
Unclassified									
110	Uncharacterized protein	195265468	E0CVH6 (53)	*Vitis vinifera*	13 (4)	33/5.67	35/5.36	–	+
111	Uncharacterized protein	195285674	A5BLT1 (64)	*Vitis vinifera*	19 (5)	36/6.16	35/7.93	–	+
112	Uncharacterized protein	195274899	F6I5L8 (92)	*Vitis vinifera*	26 (6)	31/8.77	29/6.80	–	+
113	Uncharacterized protein	195261684	A5C3G7 (91)	*Vitis vinifera*	8 (2)	30/5.89	28/6.02	–	+
114	Uncharacterized protein	195195929	F6H392 (82)	*Vitis vinifera*	14 (5)	72/5.77	72/5.17	+	–
115	Germin-like protein 5-1	195208226	Q6I544 (70)	*Oryza sativa*	17 (4)	21/7.94	29/5.57	+	–
Secondary metabolism									
116	Leucoanthocyanidin dioxygenase	195227726	Q96323 (86)	*Arabidopsis thaliana*	18(4)	40/5.23	43/5.61	–	+
117	Lactoylglutathione lyase	195231074	F6H7L5 (88)	*Vitis vinifera*	12 (3)	46/5.68	39/4.98	+	–

subunit species (spots 71, 72, 78, 79, 81, 88, 102, 106 and 107) were observed as differentially represented (generally over-represented) in inoculated *A. chinensis* shoots, as already determined in other pathosystems [10,14,16].

Plant defence from pathogens has also been associated with molecular networks based on reactive oxygen species (ROS) and phytohormone signalling [10,11,61–63]. Our results were consistent with previous observations on other pathosystems and proved a remarkable quantitative increase of proteins involved in regulation of plant redox homeostasis, such as ascorbate peroxidase (spot 84 and 85) and glutathione transferases (GSTs) species (spot 87 and 89) [10,11,16,26,45,64]. Data on GST were also confirmed at transcriptional level. Recently, the first protein has been identified as associated with resistance of tobacco plants to *P. s.* pv. *tabaci* infection [65]; similarly, GSTs were linked to early response of *A. thaliana* to *P. s.* pv. *tomato* DC3000 [24,25]. Conversely, an isoform-dependent quantitative change was observed for polyphenol oxidase (spots 73, 100 and 101), an enzyme that catalyzes the oxidation of phenolic metabolites to quinones and is also implicated in plant defence against pathogens/insects [10,66]. Its differential proteomic profile suggests the occurrence of PTM mechanisms affecting protein isoform distribution after bacterial challenge. A similar phenomenon was also observed for isoflavone reductase P3 isoforms (spots 76 and 103), whose avocado and rice protein homologues were observed as over-represented following infection with the oomycete *Phytophthora cinnamomi* and rice blast fungus, respectively [55,64]. Proteins whose concentration is increased by the abiotic stress phytohormone abscisic acid (ABA), namely annexin (spot 77 and 104) and abscisic acid stress ripening protein (spot 105) species, showed a variable quantitative trend after bacterial challenge; the first one was up-regulated, while the remaining ones were down-regulated. This contrast with previous proteomic studies on pathogen-infected plants [10,64], which suggested that enhanced ABA levels correlate with an increased plant susceptibility to pathogen attack [67–70]. Our results could be related to a peculiar behaviour of the pathosystem investigated or to the experimental conditions used in this study. Further investigations are necessary to clarify the role of ABA in *A. chinensis*/*P. s.* pv. *actinidiae* interaction.

3.3. Plant proteins involved in energy regulation

A number of proteins involved in carbohydrate metabolism, glycolysis Krebs cycle and ATP production were over-represented following *A. chinensis* inoculation. In this context, worth-mentioning are isocitrate dehydrogenase (spot 23), malate dehydrogenase (spots 24), 6-phosphogluconate dehydrogenase (spot 22), UDP-glucose 4-epimerase (spot 25), ATPase α subunit (spot 18), 6-phosphogluconolactonase 5 (spot 27), succinate dehydrogenase (spot 15) and aldehyde dehydrogenase

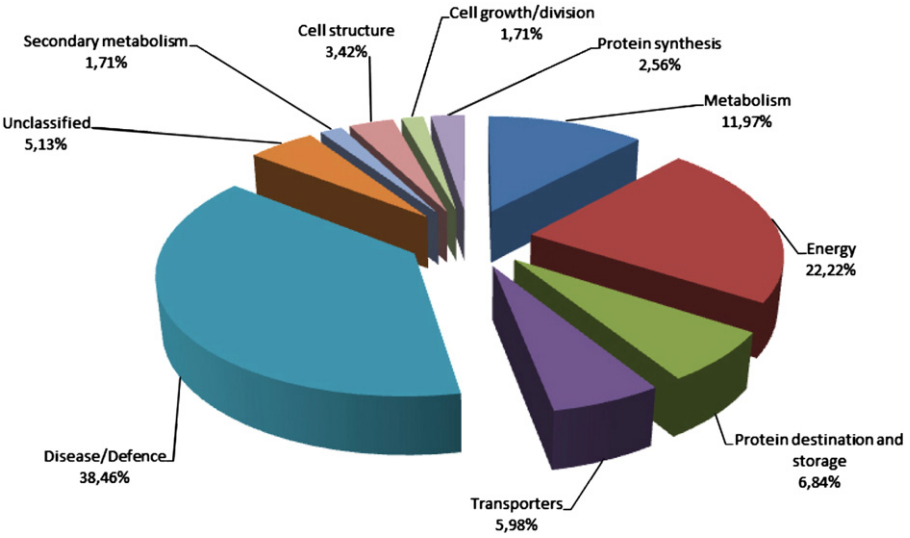

Fig. 4 – Functional classification and relative distribution of the differentially represented protein species in *A. chinensis* cv. Soreli shoots after infection with *P. syringae* pv. *actinidiae*.

(spot 20) species, which confirmed previous observations on other phatosystems [10,16,25,43,71,72]. The latter three enzymes have been reported as being related also to plant defence, since they inhibit bacterial β-lactamase or contribute to detoxify the oxidative burst caused by ROS associated with protective mechanisms [73]. Conversely, isoform-dependent quantitative changes were observed for triosephosphate isomerase (spots 28 and 39) and enolase (spots 21 and 33). Their differential proteomic profile suggests the occurrence of PTM events affecting protein isoform distribution after bacterial challenge. Finally, a down-representation of different fructokinase-2 gene products (spots 36, 37, 38), an enzyme involved in starch synthesis and water transport [74], suggested the inhibition of polysaccharide storage processes in infected plants.

On the other hand, alcohol dehydrogenase (ADH) species (spots 1, 2 and 3) were also over-represented in infected *A. chinensis* shoots; this protein is a key enzyme involved in NAD^+ production during fermentation. In this context, increasing evidences have been accumulated on the critical role of the fermentative metabolism in plant-pathogen interactions [75]. In fact, pathogen-infected leaves are characterized by augmented fluxes of carbon derivatives (generally hexoses), as observed in the barley/*Blumeria graminis* and *Arabidopsis*/*Albugo candida*

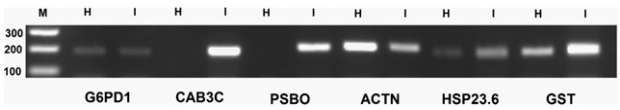

Fig. 5 – Indirect verification of the protein expression during the *A. chinensis*/*P. syringae* pv. *actinidiae* interaction through an evaluation of the corresponding transcript levels, as assessed by semiquantitative RT-PCR. PSBO, oxygen-evolving enhancer protein 1; CAB3C, chlorophyll a-b binding protein 3C; ACTN, actinidain; HSP23.6, 23.6 kDa heat shock protein; GST, glutathione S-transferase. Glucose-6-phosphate dehydrogenase (G6PD1) was used as housekeeping gene. H, healthy *A. chinensis* shoot; I, *A. chinensis* shoot infected with *P. syringae* pv. *actinidiae*.

pathosystems [76–78]. By yielding reduced ATP amounts, when compared to oxidative phosphorylation, this fermentative pathway may maintain the primary energy metabolism of the host cells under a condition of an increased metabolic flux at the site of pathogen infection.

Similarly, enzymes involved in photosynthesis and photorespiration, such as oxygen-evolving enhancer proteins 1 (spots 26), chlorophyll a-b binding protein 3C (spot 29), an isoform of oxygen-evolving enhancer proteins 2 (spots 30) and NADP-dependent malic enzyme (spots 16, 17 and 19) species increased their concentration as result of *P. s.* pv. *actinidiae* infection. Proteomic data on the first two proteins were also confirmed at transcriptional level (Fig. 5). A localized repression of photosynthetic activity is generally observed during pathogens attack to plant leaves [71,79], which parallel with down-expression of genes related to photosynthesis [10,14,18,26]. In particular, a photosynthesis rate decline was observed upon inoculation of *A. thaliana* foliage with *P. syringae* pv. *tomato* [80]. Over-representation of specific enzymes with photosynthetic activity in the shoot, as described in this study, may be explained on the basis of the dynamic wilting process affecting kiwi foliage. Thus, it is conceivable that the shoots, even though sustaining a pathogen attack, continue to act as a mandatory source for the plant, trying to provide the assimilates otherwise yielded by the healthy leaves. This issue would represent a novelty in deciphering the composite scenario intervening in the different plant organs during pathogen infection, which would simply imply a reprogramming of the shoot metabolism following systemic bacterial invasion and resulting leaf wilting. In this context, an increased photosynthetic activity was recently described in the shoots of *Arabidopsis halleri*, when grown in presence of Cd, Zn and various bacterial strains [81].

3.4. *Plant proteins involved in other molecular pathways*

While proteins assisting polypeptide synthesis and folding, such as eukaryotic initiation factors (spots 43 and 45), ribosomal proteins (spot 44), NAC subunit α (spot 56), HSPs (see previous

chapter) and protein disulfide isomerase (spot 47) species, were over-represented after bacterial challenge, those facilitating their degradation, i.e. various proteases/peptidases (spots 34, 35, 50–53), showed an opposite trend. These findings suggest that *A. chinensis* metabolism during *P. s.* pv. *actinidiae* attack is directed toward ensuring all key molecules (proteins) and metabolic pathways, including those related to energy regulation and defence mechanisms, essential to promote plant surviving potential. Cell growth/division seems also promoted in infected shoots by over-expression of cell division protein and histone gene products (spots 41 and 42).

Depending on their nature, enzymes involved in amino acid and nucleotide metabolism presented a variable quantitative behaviour. In fact, fumarylacetoacetate hydrolase (spot 7), catalyzing the degradation of tyrosine, glutamine synthetase (spot 4), and adenosine kinase 2 (spot 5 and 6), involved in adenosine re-cycling, showed an increased concentration in infected *A. chinensis* shoots. Conversely, methylenetetrahydrofolate reductase (spot 8), glutamate dehydrogenase A and B (spots 10 and 11), adenosylhomocysteinase (spot 9), thiosulphate sulfurtransferase (spot 13), nucleoside diphosphate kinase (spot 14) and patatin-like protein (PLP) 3 (spot 12) species were down-represented. PLPs play an essential role in cell death execution and differentially affect oxylipins biosynthesis and resistance to pathogens [82]. Quantitative trends observed for some of these enzymes were also observed in other pathosystems [10,26].

Finally, various studies have demonstrated that plant resistance to bacterial infection correlates with their content in secondary metabolites, i.e. flavonoids, phytoalexins, and glycoalkaloids [10,16,64]. Anthocyanins, for example, seem to play a defensive role during pathogen attack by exerting their toxic potential [83,84]. Accordingly, we found an over-representation of a leucoanthocyanidin dioxygenase species (spot 116) in the infected shoots; this enzyme is involved in proantocyanidine biosynthesis. By increasing the concentration of toxic methylglyoxal [85], reduced amounts of a lactoylglutathione lyase gene product (spot 117) were analogously detected in inoculated shoots. A number of non-characterized plant proteins were also ascertained as differentially represented following bacterial infection.

3.5. *Bacterial proteins*

Our proteomic analysis also revealed the occurrence of a bacterial protein species (spot 54) in infected shoots, which was identified as outer membrane porin F (ompF). A protein of this class was already identified in other pathosystems, such as the *Passiflora edulis/Xanthomonas axonopodis* pv. *passiflorae* [86] and *Saintpaulia ionantha/Dickeya dadanthii* ones [87], when bacterial culture media were added with host leaf extracts and the bacterial proteome was subsequently assessed. *P. s. pv. syringae* OmpF homologue resides in a gene cluster eliciting plant hypersensitive response, a molecular phenomenon generally considered to be a manifestation of recognition and resistance [88]. Recently, this porin was demonstrated to be an essential factor for *P. aeruginosa* virulence toward mammals, at least partly through modulation of the quorum-sensing network [89]. Its further characterization is needed, together with transcriptomic studies aiming at assaying its expression during the initial events of plant colonization. Its use for early detection of the pathogen in the kiwifruit propagation material may provide a valid tool for certification schemes, currently required for global circulation of kiwifruit scions, and grafted or self-rooted plants.

4. Conclusions

Plant–bacteria interactions are highly complex since multiple bacterial factors and plant-signalling events take place, which ultimately define the susceptibility or resistance of the plant exposed to the pathogen. Current investigations are directed towards gaining a better understanding of the molecular mechanisms implicated in basal and specific plant defence responses against plant bacterial pathogens. In this context, detailed proteomic comparisons of microbe-challenged and control plants have allowed the identification of novel protein species whose biological role warrants in-depth biochemical and cellular elucidation [10–12]. In the current study, we performed a comparative proteomic analysis of *A. chinensis* shoot tissues before and following inoculation with the pandemic *P. s.* pv. *actinidiae* to elucidate molecular mechanisms underlying this plant–microbe interaction. Although gel-based proteomic investigations present well-known limitations [90], this study identified a number of differentially represented gene products in infected shoots. Proteins related to plant protection, such as PR polypeptides or components involved in basal protection, oxidative stress, heat shock, and related transport and signalling processes, were characterized as the most represented category of induced species. Proteins involved in carbohydrate metabolism and energy regulation were also differentially represented upon infection. A bacterial outer membrane protein was identified as well; its further characterization in the very early phases of the host colonization will help detecting *P. s.* pv. *actinidiae* in kiwifruit propagative material.

Similarly to what ascertained in previous studies on other plant organs infected by pathogenic bacteria and fungi [10,11], our results suggest a general reprogramming of the shoot metabolism in the *A. chinensis/P. s.* pv. *actinidiae* pathosystem. These molecular events parallel systemic pathogen colonization of the host, dynamically involving leaf wilting, root infection and shoot canker formation. Further investigations, based on advanced proteomic techniques, i.e. quantitative gel-free approaches, or directed to specific sub-cellular compartments, are necessary to provide a better comprehension of the molecular mechanisms implicated in kiwi plant response to pathogen invasion. These studies will identify promising novel targets for the development of cultivars with improved disease resistance.

Supplementary data to this article can be found online at http://dx.doi.org/10.1016/j.jprot.2012.10.014.

Acknowledgments

This study was supported by dedicated grants from the Italian Ministry of Agriculture, Food and Forestry project “Interventi di coordinamento ed implementazione delle azioni di ricerca, lotta e difesa al cancro batterico dell’Actinidia” to MS and

from the Italian Ministry of Economy and Finance project "Innovazione e sviluppo del Mezzogiorno - Conoscenze Integrate per Sostenibilità ed Innovazione del Made in Italy Agroalimentare" Legge n.191/2009 to AS.

REFERENCES

[1] Scortichini M, Marcelletti S, Ferrante P, Petriccione M, Firrao G. *Pseudomonas syringae* pv. *actinidiae*: a re-emerging, multi-faceted, pandemic pathogen. Mol Plant Pathol 2012, http://dx.doi.org/10.1111/J.1364-3703.2012.00788.X.
[2] Ferrante P, Scortichini M. Molecular and phenotypic features of *Pseudomonas syringae* pv. *actinidiae* isolated during recent epidemics of bacterial canker of yellow kiwifruit (*Actinidia chinensis*) in central Italy. Plant Pathol 2010;59:954-62.
[3] Gallelli A, L'Aurora A, Loreti S. Gene sequence analysis for the molecular detection of *Pseudomonas syringae* pv. *actinidiae*: developing diagnostic protocols. J Plant Pathol 2011;93:425-35.
[4] Marcelletti S, Ferrante P, Petriccione M, Firrao G, Scortichini M. *Pseudomonas syringae* pv. *actinidiae* draft genomes comparison reveal strain-specific features involved in adaptation and virulence to *Actinidia* species. PLoS One 2011;6:e27297.
[5] Mazzaglia A, Studholme DJ, Taratufolo MC, Cai R, Almeida NF, Goodman T, et al. *Pseudomonas syringae* pv. *actinidiae* (PSA) isolates from recent bacterial canker of kiwifruit outbreaks belong to the same genetic lineage. PLoS One 2012;7:e36518.
[6] Ferrante P, Fiorillo E, Marcelletti S, Marocchi F, Mastroleo M, Simeoni S, et al. The importance of the main colonization and penetration sites of *Pseudomonas syringae* pv. *actinidiae* and prevailing weather conditions in the development of epidemics in yellow kiwifruit. J Plant Pathol 2012;94:455-61.
[7] Serizawa S, Ichikawa T. Epidemiology of bacterial canker of kiwifruit. Infection and bacterial movement in tissue of new canes. Ann Phytopathol Soc Jpn 1993;59:452-9.
[8] Spinelli F, Donati I, Vanneste JL, Costa M, Costa G. Real time monitoring of the interactions between *Pseudomonas syringae* pv. *actinidiae* and *Actinidia* species. Acta Horticult 2011;913:461-5.
[9] Cheng Z, Woody ZO, Glick RB, McConkey JB. Characterization of Plant-Bacterial Interactions Using Proteomic Approaches. Curr Proteomics 2010;7:244-57.
[10] Afroz A, Ali GM, Mir A, Komatsu S. Application of proteomics to investigate stress-induced proteins for improvement in crop protection. Plant Cell Rep 2011;30:745-63.
[11] Zimaro T, Gottig N, Garavaglia BS, Gehring C, Ottado J. Unraveling plant responses to bacterial pathogens through proteomics. J Biomed Biotechnol 2011:354801.
[12] Gonzalez-Fernandez R, Jorrin-Novo JV. Contribution of proteomics to the study of plant pathogenic fungi. J Proteome Res 2012;11:3–16.
[13] Mehta A, Brasileiro ACM, Souza DSL, Romano E, Campos MA, Grossi-da-Sa MF, et al. Plant–pathogen interactions: what is proteomics telling us? FEBS J 2008;275:3731-46.
[14] Ji X, Gai Y, Zheng C, Mu Z. Comparative proteomic analysis provides new insights into mulberry dwarf responses in mulberry (*Morus alba* L.). Proteomics 2009;9:5328-39.
[15] Quirino BF, Candido ES, Campos PF, Franco OL, Kruger RH. Proteomic approaches to study plant-pathogen interactions. Phytochemistry 2010;71:351-62.
[16] Margaria P, Palmano S. Response of the *Vitis vinifera* L. cv. 'Nebbiolo' proteome to Flavescence dorée phytoplasma infection. Proteomics 2011;11:212-24.
[17] Taheri F, Nematzadeh G, Zamharir MG, Nekouei MK, Naghavi M, Mardi M, et al. Proteomic analysis of the Mexican lime tree response to "Candidatus Phytoplasma aurantifolia" infection. Mol Biosyst 2011;7:3028-35.
[18] Mahmoud T, Jan A, Kakishima M, Komatsu S. Proteomic analysis of bacterial-blight defense-responsive proteins in rice leaf blades. Proteomics 2006;6:6053-65.
[19] Zamany A, Liu JJ, Ekramoddoullah AK. Comparative proteomic profiles of *Pinus monticola* needles during early compatible and incompatible interactions with *Cronartium ribicola*. Planta 2012, http://dx.doi.org/10.1007/s00425-012-1715-x.
[20] Rampitsch C, Bykova NV, McCallum B, Beimcik E, Ens W. Analysis of the wheat and *Puccinia triticina* (leaf rust) proteomes during a susceptible host-pathogen interaction. Proteomics 2006;6:1897-907.
[21] Andrade AE, Silva LP, Pereira JL, Noronha EF, Reis Jr FB, Bloch Jr C, et al. *In vivo* proteome analysis of *Xanthomonas campestris* pv. *campestris* in the interaction with the host plant *Brassica oleracea*. FEMS Microbiol Lett 2008;81:167-74.
[22] Garavaglia BS, Thomas L, Zimaro T, Gottig N, Daurelio LD, Ndimba B, et al. A plant natriuretic peptide-like molecule of the pathogen *Xanthomonas axonopodis* pv. *citri* causes rapid changes in the proteome of its citrus host. BMC Plant Biol 2010;10:51.
[23] Widjaja I, Lassowskat I, Bethke G, Eschen-Lippold L, Long HH, Naumann K, et al. A protein phosphatase 2C, responsive to the bacterial effector AvrRpm1 but not to the AvrB effector, regulates defense responses in *Arabidopsis*. Plant J 2010;61: 249-58.
[24] Jones AME, Thomas V, Truman B, Lilley K, Mansfield J, Grant M. Specific changes in the *Arabidopsis* proteome in response to bacterial challenge: differentiating basal and R-gene mediated resistance. Phytochemistry 2004;65:1805-16.
[25] Jones AME, Thomas V, Bennett MH, Mansfield J, Grant M. Modifications to the Arabidopsis defense proteome occur prior to significant transcriptional change in response to inoculation with *Pseudomonas syringae*. Plant Physiol 2006;142: 1603-20.
[26] Holzmeister C, Fröhlich A, Sarioglu H, Bauer N, Durner J, Lindermayr C. Proteomic analysis of defense response of wildtype *Arabidopsis thaliana* and plants with impaired NO- homeostasis. Proteomics 2011;11:1664-83.
[27] Campos A, Goncalo da Costa GD, Coelho AV, Fevereiro P. Identification of bacterial protein markers and enolase as a plant response protein in the infection of *Olea europaea* subsp. *europaea* by *Pseudomonas savastanoi* pv. savastanoi. Eur J Plant Pathol 2009;125:603-16.
[28] Dahal D, Pich A, Braun HP, Wydra K. Analysis of cell wall proteins regulated in stem of susceptible and resistant tomato species after inoculation with *Ralstonia solanacearum*: a proteomic approach. Plant Mol Biol 2010;73: 643-58.
[29] Kurkcuoglu S, Piotrowski M, Gau AE. Up-regulation of pathogenesis related proteins in the apoplast of *Malus domestica* after application of a non-pathogenic bacterium. J Biosci 2004;59:843-8.
[30] Kandasamy S, Loganathan K, Muthuraj R, Duraisamy S, Seetharaman S, Thiruvengadam R, et al. Understanding the molecular basis of plant growth promotional effect of *Pseudomonas fluorescens* on rice through protein profiling. Proteome Sci 2009;7:1-7.
[31] Crowhurst RN, Gleave AP, MacRae EA, Ampomah-Dwamena C, Ross G, Atkinson RG, et al. Analysis of expressed sequence tags from *Actinidia*: applications of a cross species EST database for gene discovery in the areas of flavor, health, color and ripening. BMC Genomics 2008;9:351.
[32] Buell CR, Joardar V, Lindeberg M, Selengut J, Paulsen IT, Gwinn ML, et al. The complete genome sequence of the Arabidopsis and tomato pathogen *Pseudomonas syringae* pv. *tomato* DC3000. Proc Natl Acad Sci U S A 2003;100: 10181-6.

[33] Feil H, Feil WS, Chain P, Larimer F, Di Bartolo G, Copeland A, et al. Comparison of the complete genome sequences of *Pseudomonas syringae* pv. *syringae* B728a and pv. tomato DC3000. Proc Natl Acad Sci U S A 2005;102:11064-9.
[34] Joardar V, Lindeberg M, Jackson RW, Selengut J, Dodson R, Brinkac LM, et al. Whole-genome sequence analysis of *Pseudomonas syringae* pv. phaseolicola 1448A reveals divergence among pathovars in genes involved in virulence and transposition. J Bacteriol 2005;187:6488-98.
[35] Ferrante P, Scortichini M. Identification of *Pseudomonas syringae* pv. *actinidiae* as causal agent of bacterial canker of yellow kiwifruit (*Actinidia chinensis* Planchon) in Central Italy. J Phytopathol 2009;157:768-70.
[36] Wang W, Scali M, Vignani R, Spadafora A, Sensi E, Mazzuca S, et al. Protein extraction for two dimensional electrophoresis from olive leaf, a plant tissue containing high level of interfering compounds. Electrophoresis 2003;24:2369-75.
[37] Bradford MM. A rapid and sensitive method for the quantitation of microgram quantities of protein utilizing the principle of protein-dye binding. Anal Biochem 1976;72: 248-54.
[38] Rocco M, Corrado G, Arena S, D'Ambrosio C, Tortiglione C, Sellaroli S, et al. The expression of tomato prosystemin gene in tobacco plants highly affects host proteomic repertoire. J Proteomics 2008;71:176-85.
[39] Corrado G, Alagna F, Rocco M, Renzone G, Varricchio P, Coppola V, et al. Molecular interaction between the olive and the fruit fly *Bactrocera oleae*. BMC Plant Biol 2012;12:86.
[40] Rozen S, Skaletsky H. Primer3 on the WWW for general users and for biologist programmers. Methods Mol Biol 2000;132: 365-86.
[41] Bevan M, Bancroft I, Bent E, Love K, Goodman H, Dean C, et al. Analysis of 1.9 Mb of contiguous sequence from chromosome 4 of *Arabidopsis thaliana*. Nature 1998;391:485-8.
[42] Roberts TH, Hejgaard J. Serpins in plants and green algae. Funct Integr Genomics 2008;8:1–27.
[43] Fan J, Chen C, Yu Q, Brlansky RH, Li ZG, Gmitter Jr FG. Comparative iTRAQ proteome and transcriptome analyses of sweet orange infected by "Candidatus Liberibacter asiaticus". Physiol Plant 2011;143:235-45.
[44] Zhou L, Cheung MY, Li MW, Fu Y, Sun Z, Sun SM, et al. Rice hypersensitive induced reaction protein 1 (OsHIR1) associates with plasma membrane and triggers hypersensitive cell death. BMC Plant Biol 2010;10:290.
[45] Chen F, Yuan Y, Li Q, He Z. Proteomic analysis of rice plasma membrane reveals proteins involved in early defense response to bacterial blight. Proteomics 2007;7:1529-39.
[46] Van Loon LC, Rep M, Pieterse CMJ. Significance of inducible defense-related proteins in infected plants. Annu Rev Phytopathol 2006;44:135-62.
[47] Kim ST, Cho KS, Yu S, Kim SG, Hong JC, Han CD, et al. Proteomic analysis of differentially expressed proteins induced by rice blast fungus and elicitor in suspension-cultured rice cells. Proteomics 2003;23:68-78.
[48] Van Kan JAL, Joosten MHAJ, Wagemakers CAM, Berg-Welthuis GCM, Wit PJGM. Differential accumulation of mRNAs encoding extracellular and intracellular PR proteins in tomato induced by virulent and avirulent races of *Cladosporium fulvum*. Plant Mol Biol 1992;20:513-27.
[49] Saizer P, Bonanomi A, Beyer K, Vogeli-Lange R, Aeschbacher RA, Lange J, et al. Differential expression of eight chitinase genes in *Medicago truncatula* roots during mycorrhiza formation, nodulation, and pathogen infection. Mol Plant Microbe Interact 2000;13:763-77.
[50] Dana MLM, Pintor-Toro JA, Cubero B. Transgenic tobacco plants overexpressing chitinases of fungal origin show enhanced resistance to biotic and abiotic stress agents. Plant Physiol 2006;142:722-30.
[51] Dafoe NJ, Gowen BE, Constabel CP. Thaumatin-like proteins are differentially expressed and localized in phloem tissues of hybrid poplar. BMC Plant Biol 2010;10:191.
[52] Wang X, Liu W, Chen X, Tang C, Dong Y, Ma J. Differential gene expression in incompatible interaction between wheat and stripe rust fungus revealed by cDNA-AFLP and comparison to compatible interaction. BMC Plant Biol 2010;10:9.
[53] Anzlovar S, Dermastia M. The comparative analysis of osmotins and osmotins-like PR-5 proteins. Plant Biol 2003;5: 116-24.
[54] Hauser M, Egger M, Wallner M, Wopfner N, Schmidt G, Ferreira F. Molecular properties of plant food allergens: a current classification into protein families. Open Immunol J 2008;1:1–12.
[55] Kim ST, Cho KS, Yu S, Kim SG, Hong JC, Han CD, et al. Proteomic analysis of differentially expressed proteins induced by rice blast fungus and elicitor in suspension-cultured rice cells. Proteomics 2003;3:2368-78.
[56] Park CJ, Kim KJ, Shin R, Park JM, Paek KH. Pathogenesis-related protein 10 isolated from hot pepper functions as a ribonuclease in an antiviral pathway. Plant J 2004;37:186-98.
[57] Noel LD, Cagna G, Stuttman J, Wirthmuller L, Betsuyaku S, Witte C-P, et al. Interaction between SGT1 and cytosolic/nuclear HSC70 chaperones regulates *Arabidopsis* immune responses. Plant Cell 2007;19:4061-76.
[58] Jelenska J, van Hal JA, Greenberg JT. *Pseudomonas syringae* hijacks plant stress machinery for virulence. Proc Natl Acad Sci U S A 2010;107:13177-82.
[59] Sullivan JA, Shirasu K, Deng XW. The diverse role of ubiquitin and the 26S proteasome in the life of plants. Nat Rev 2003;4: 948-58.
[60] Citovsky V, Zaltsman A, Kozlovsky SV, Gafni Y, Krichevsky A. Proteasomal degradation in plant-pathogen interactions. Semin Cell Dev Biol 2009;20:1048-54.
[61] Van Breusegem F, Dat JF. Reactive oxygen species in plant cell death. Plant Physiol 2006;141:404-11.
[62] Moons A, Gerald L. Regulatory and functional interactions of plant growt regulators and plant glutathione S-transferases (GSTs). In: Litwack G, editor. Vitamins and Hormones, vol. 72. New York: Academic; 2005. p. 155-202.
[63] Fones H, Preston G. Reactive oxygen and oxidative stress tolerance in plant pathogenic Pseudomonas. FEMS Microbiol Lett 2011;327:1-8.
[64] Acosta-Muñiz CH, Escobar-Tovar L, Valdes-Rodríguez S, Fernández-Pavia S, Arias-Saucedo LJ, de la Cruz Espindola Barquera M, et al. Identification of avocado (*Persea americana*) root proteins induced by infection with the oomycete *Phytophthora cinnamomi* using a proteomic approach. Physiol Plant 2012;144:59-72.
[65] Faize M, Burgos L, Faize L, Petri C, Barba-Espin G, Diaz-Vivancos P, et al. Modulation of tobacco bacterial disease resistance using cytosolic ascorbate peroxidase and Cu,Zn-superoxide dismutase. Plant Pathol 2011, http://dx.doi.org/10.1111/j.1365-3059.2011.02570.x.
[66] Thipyapong P, Stout MJ, Attajarusit J. Functional analysis of polyphenol oxidases by antisense/sense technology. Molecules 2007;12:1569-95.
[67] Audenaert K, De Meyer GB, Hofte M. Abscisic acid determines basal susceptibility of tomato to *Botrytis cinerea* and suppresses salicylic acid-dependent signalling mechanism. Plant Physiol 2002;128:491-501.
[68] Mohr PG, Cahill PM. Abscisic acid influences the susceptibility of Arabidopsis thaliana to *Pseudomonas syringae* pv. *tomato* and *Peronospora parasitica*. Funct Plant Biol 2003;30:461-9.
[69] Thaler J, Bostock R. Interactions between abscisic-acid-mediated responses and plant resistance to pathogens and insects. Ecology 2004;85:48-58.

[70] Mauch-Mani B, Mani F. The role of abscisic acid in plant-pathogen interaction. Curr Opin Plant Biol 2005;8: 409-14.
[71] Berger S, Sinha AK, Roitsch T. Plant physiology meets phytopathology: plant primary metabolism and plant-pathogen interaction. J Exp Bot 2007;58:4019-26.
[72] Garavaglia BS, Thomas L, Gottig N, Zimaro T, Garofalo CG, Gehring C, et al. Shedding light on the role of photosynthesis in pathogen colonization and host defense. Comm Int Biol 2010;3:382-4.
[73] Sunkar R, Bartels D, Kirch HH. Overexpression of a stress-inducible aldehyde dehydrogenase gene from *Arabidopsis thaliana* in transgenic plants improves stress tolerance. Plant J 2003;35:452-4.
[74] German MA, Dai N, Matsevitz T, Hanael R, Petreikov M, Bernstein M, et al. Suppression of fructokinase encoded by *LeFRK2* in tomato stem inhibits growth and causes wilting of young leaves. Plant J 2003;34:837-46.
[75] Wildermuth MC. Modulation of host nuclear ploidy: a common plant biotroph mechanism. Curr Opin Plant Biol 2010;13:1–10.
[76] Chou H-M, Bundock N, Rolfe SA, Scholes JD. Infection of Arabidopsis thaliana leaves with *Albugo candida* white blister rust causes a reprogramming of host metabolism. Mol Plant Pathol 2000;1:99–113.
[77] Swarbrick PJ, Schulze-Lefert P, Scholes JD. Metabolic consequences of susceptibility and resistance in barley leaves challenged with powdery mildew. Plant Cell Environ 2006;29:1071-6.
[78] Proels RK, Westermeier W, Huckeloven R. Infection of barley with the parasitic fungus *Blumeria graminis* f. sp. *hordei* results in the induction of HvADH1 and HvADH2. Plant Signal Behav 2001;6:1584-7.
[79] Bolton MD. Primary metabolism and plant defense-fuel for the fire. Mol Plant Microbe Interact 2009;22:487-97.
[80] Bonfig KB, Schreiber U, Gabler A, Roitsch T, Berger S. Infection with virulent and avirulent *Pseudomonas syringae* differentially affects photosynthesis and sink metabolism in *Arabidopsis* leaves. Planta 2006;225:1–12.
[81] Farinati S, Dal Corso G, Bona E, Corbella M, Lampis S, Cecconi D, et al. Proteomic analysis of *Arabidopsis halleri* shoots in response to the heavy metals cadmium and zinc and rhizosphere microorganisms. Proteomics 2009;9:4837-50.
[82] La Camera S, Balagué C, Göbel C, Geoffroy P, Legrand M, Feussner I, et al. The *Arabidopsis* patatin-like protein 2 (PLP2) plays an essential role in cell death execution and differentially affects biosynthesis of oxylipins and resistance to pathogens. Mol Plant Microbe Interact 2009;22:469-81.
[83] Lorenc-Kukula K, Zuk M, Kulma A, Czemplik M, Kostyn K, Skala J, et al. Engineering flax with the GT family 1 *Solanum sogarandinum* glycosyltransferase SsGT1 confers increased resistance to *Fusarium* infection. J Agric Food Chem 2009;57: 6698-705.
[84] Vega A, Gutiérrez RA, Peña-Neira A, Cramer GR, Arce-Johnson P. Compatible GLRaV-3 viral infections affect berry ripening decreasing sugar accumulation and anthocyanin biosynthesis in *Vitis vinifera*. Plant Mol Biol 2011;77:261-74.
[85] Lin F, Xu J, Shi J, Li H, Li B. Molecular cloning and characterization of a novel glyoxalase I gene TaGly I in wheat (*Triticum aestivum* L.). Mol Biol Rep 2010;37:729-35.
[86] Tahara ST, Metha A, Rosato YB. Proteins induced by *Xanthomonas axonopodis* pv. *passiflorae* with leaf extract of the host plant (*Passiflorae edulis*). Proteomics 2003;3:95–102.
[87] Babujee L, Venkatesh B, Yamazaki A, Tsuyumu S. Proteomic analysis of the carbonate insoluble outer membrane fraction of the soft-rot pathogen *Dickeya dadantii* (syn. *Erwinia chrysanthemi*) strain 3937. J Proteome Res 2007;6:62-9.
[88] Li TH, Benson SA, Hutcheson SW. Phenotypic expression of the *Pseudomonas syringae* pv. syringae 61 hrp/hrm gene cluster in *Escherichia coli* MC4100 requires a functional porin. J Bacteriol 1992;174:1742-9.
[89] Fito-Boncompte L, Chapalain A, Bouffartigues E, Chaker H, Lesouhaitier O, Gicquel G, et al. Full virulence of *Pseudomonas aeruginosa* requires OprF. Infect Immun 2011;79:1176-86.
[90] Lopez JL. Two-dimensional electrophoresis in proteome expression analysis. J Chromatogr B 2007;849:190-202.